

# Studies on the Transesterification of Glycerides: I. The Methanolysis of Tripalmitin Catalysed by Diorganotin(IV) Compounds

Chai Hon Yean and V. G. Kumar Das\*

Department of Chemistry, University of Malaya, 50603 Kuala Lumpur, Malaysia

The potential of diorganotin compounds, in particular alkoxides and phenoxides, to function as neutral and non-corrosive catalysts in the methanolysis of tripalmitin (the main triglyceride in palm oil) to methyl palmitate has been investigated. The compounds reveal a strong dependence of catalytic activity on the nature of the organic moiety on tin, the ring-borne substituent on the phenoxyl group and the chain length of the alkoxyl fragment, as well as the ring size in cyclic alkoxides derived from bifunctional ligands such as diethanolamine. Kinetic studies, based on detailed compositional analysis of the reaction mixture by gas chromatography, were performed typically at  $70.0 \pm 0.1^\circ\text{C}$  in mixed methanol–tetrahydrofuran (3:2, v/v) medium and at 1.0 mol% catalyst concentration with respect to tripalmitin. The catalysts used for the kinetic studies were dibutyl bis(*p*-chlorophenoxyl)tin 1, dibutyl bis(phenoxyl)tin 2, 1,1-dibutyl-5-aza-2,8-dioxo-1-stannacyclo-octane 3, 2,2-dibutyl-2-stanna-1,3-benzdioxane 4 and dioctyltin oxide 5. The methanolysis was shown to proceed by a consecutive reaction pathway. Numerical analysis of the rate data yielded values of the three rate constants  $k_1$ ,  $k_2$  and  $k_3$  corresponding to the respective conversions, tripalmitin  $\rightarrow$  dipalmitin  $\rightarrow$  monopalmitin  $\rightarrow$  glycerol. Based on  $t_{1/2}$  values ranging from 7.2 to  $22.3\text{ h}^{-1}$ , the following order of catalytic activity was established:  $1 > 2 > 3 \gg 5 \gg 4$ ; for catalyst 4 the  $t_{1/2}$  value was close to that of the uncatalysed reaction. A six-fold increase in rate was observed when the catalyst concentration was raised from 1.0 to 3.0 mol% for 3.  $^{119}\text{Sn}$  NMR analysis of the chloroform extracts of the pot residue following solvent removal at the end of 24 h of the

transesterification reaction revealed that the catalysts 1 and 3 essentially retained their chemical integrity. Copyright © 2000 John Wiley & Sons, Ltd.

**Keywords:** transesterification; methanolysis; tripalmitin; consecutive reaction; kinetics; organotin catalysts; diorganotin alkoxide; diorganotin phenoxide

Received 20 May 1999; accepted 1 October 1999

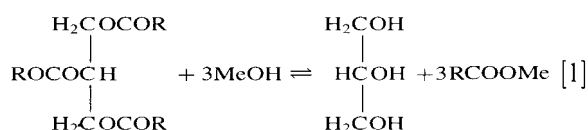
## INTRODUCTION

Transesterification, in its broadest sense, refers to a number of catalytic reactions between an ester and an acid, an alcohol or another ester, to produce esters differing in composition from the original one. Transesterification of vegetable oils with monohydric alcohols has long been an established method for the preparation of fatty acid alkyl esters which are important feedstocks in the production of fatty alcohols required for the manufacture of surfactants, stabilizers and lubricants.<sup>1</sup> Recently, fatty acid methyl esters derived from the methanolysis of palm oil have been shown to function as an excellent substitute for diesel fuel,<sup>2,3</sup> possessing the attributes of high combustion efficiency and reduced emission of carbon monoxide in the exhaust even when used as blends with conventional diesel fuel.

The catalysts traditionally used for the transesterification reactions have been mineral acids<sup>4</sup> (typically sulphuric acid), alkalis<sup>4,5</sup> (sometimes advantageously in the co-presence of quaternary ammonium salts<sup>6</sup>) and alkali-metal oxides.<sup>7</sup> These, however, suffer from such drawbacks as corrosion of processing equipment, dehydration of alcohols, isomerization of unsaturated fatty acids, soap formation etc. To overcome these problems, new

\* Correspondence to: V. G. Kumar Das, Department of Chemistry, University of Malaya, 50603 Kuala Lumpur, Malaysia.  
Contract/grant sponsor: National Science Council; Contract/grant number: IRPA 2-07-04-06.

catalyst systems continue to be intensively investigated, and among the noteworthy examples here are guanidine and its derivatives,<sup>7,8</sup> and the enzyme lipase.<sup>9,10</sup> Organotin compounds appear not to have been used yet in studies with triglycerides, although their catalytic potential in the transesterification of acetates and propionates,<sup>11–13</sup> methacrylates,<sup>14,15</sup> dialkyl carbonates<sup>16,17</sup> and other esters<sup>18–20</sup> has been documented. This has prompted the present investigation of their use for catalysing the methanolysis of tripalmitin, the dominant triglyceride in palm oil (Eqn [1]; R = C<sub>15</sub>H<sub>31</sub>).



As indicated in Eqn [1], a 3:1 molar ratio of alcohol to triglyceride is required for the reaction on the basis of stoichiometry. However, Bradshaw and co-workers,<sup>21</sup> in studies on vegetable oils using alkali catalysts, have reported that practical conversion yields of 98% can only be achieved with a molar ratio of 4.8:1. Others, in particular Feuge and Gros<sup>22</sup> and Lehman and Gauglitz,<sup>23</sup> have advocated a 6:1 molar ratio; molar ratios higher than this, according to these authors, tended to hamper recovery of ester and glycerol. In this study, which was also aimed at understanding the mechanism of the tripalmitin conversion, we have used an excess of the methanolic reagent so as to simplify the kinetics as well as favouring the equilibrium towards product (methyl palmitate) formation.

## EXPERIMENTAL

### Reagents and reference standards

High-purity (99%) grades of mono-, di- and tripalmitin (Sigma), triacontane (Aldrich) and methyl palmitate (Fluka) were used as reference standards. Tripalmitin ( $\geq 95\%$ ) for the methanolysis reaction (Fluka), bis(trimethylsilyl)trifluoroacetamide (BSTFA) (Tokyo Kasei, Japan), dibutyltin oxide (Organotin Chemie, Germany), dioctyltin oxide (a gift from Witco, Germany), and all other chemicals used in the preparation of the diorganotin catalysts such as monohydric alcohols, ethylene glycol, phenols, diethanolamine etc., were commercial samples of reagent grade purity ( $>97\%$ ). Absolute

methanol was obtained by distilling AR-grade methanol following treatment with magnesium as described by Vogel.<sup>24</sup> It was stored over molecular sieves (3 Å).

### Preparation of diorganotin alkoxides and phenoxides

These were prepared by heating a mixture of the diorganotin oxide (suspended in 50 ml of tetralin or toluene) and the stoichiometric amount of alcohol or phenol under reflux for 3 h using a Dean and Stark apparatus until a homogeneous solution resulted with no further evolution of water. The solvent was then distilled off under reduced pressure to yield the product. Table 1 lists the range of products thus synthesized, all of which gave a satisfactory elemental analysis. The products were generally stored in air-tight sample bottles before use.

### Gas-chromatographic analysis

A Shimadzu GC-9A fitted with flame-ionization detector was used for gas-chromatographic analysis. The column (0.5 m  $\times$  3 mm i.d., 3% OV-1 stationary phase on 100/120 Supelcoport support material)<sup>25</sup> was conditioned overnight at 340 °C to obtain a good and stable baseline. Oxygen-free nitrogen (flow rate 57.0 ml min<sup>-1</sup>) was used as carrier gas. Optimal signals were obtained by applying an air/H<sub>2</sub> ratio of 1:1.3 throughout the analysis. Other controlled parameters were: injector temperature, 340.0 °C; oven temperature programming, 110–320 °C at 25 °C min<sup>-1</sup>, then held at 320 °C for 4 min; chart speed, 3.5 cm min<sup>-1</sup>.

### Calibration graphs, precision and limits of detection

A set of seven standard mixtures, each containing tripalmitin (TP), dipalmitin (DiP), monopalmitin (MoP) and methyl palmitate (MeP), was prepared from the respective pure component stock solutions of TP (10.0 mM), DiP (10.0 mM), MoP (10.0 mM) and MeP (50.0 mM) in chloroform. The standard mixtures were in the concentration range 5.00–0.25 mM for each of TP, DiP and MoP and 25.00–1.25 mM for MeP, and each standard mixture contained 1.0 mM triacontane as internal standard. Thus appropriate volumes of the stock solutions from 0.05 to 1.00 ml were pipetted into seven respective 7-ml vials and the solvent was then completely removed from each vial by evaporation

**Table 1** Product composition analysis for the methanolysis of tripalmitin catalysed by 3.0 mol% diorganotin<sup>a</sup>

Catalyst No.	Catalyst	Product (%)				
		Unreacted TP (%) (A)	DiP (B)	MoP (C)	Glycerol	
					Indirect estimate <sup>b</sup>	Direct estimate <sup>c</sup>
1	Bu <sub>2</sub> Sn(O(CH <sub>2</sub> ) <sub>3</sub> CH <sub>3</sub> ) <sub>2</sub>	0.23	8.69	23.48	67.60	62.4
2	Bu <sub>2</sub> Sn(O(CH <sub>2</sub> ) <sub>4</sub> CH <sub>3</sub> ) <sub>2</sub>	0.58	11.81	29.60	58.01	60.7
3	Bu <sub>2</sub> Sn(O(CH <sub>2</sub> ) <sub>5</sub> CH <sub>3</sub> ) <sub>2</sub>	1.28	16.40	34.67	47.64	51.9
4	Bu <sub>2</sub> Sn(O(CH <sub>2</sub> ) <sub>6</sub> CH <sub>3</sub> ) <sub>2</sub>	2.06	19.76	36.90	41.27	43.9
5	Bu <sub>2</sub> Sn(O(CH <sub>2</sub> ) <sub>7</sub> CH <sub>3</sub> ) <sub>2</sub>	2.48	19.36	40.66	37.49	39.3
6	Bu <sub>2</sub> Sn(O(CH <sub>2</sub> ) <sub>9</sub> CH <sub>3</sub> ) <sub>2</sub>	4.28	25.61	47.31	22.79	24.7
7	Bu <sub>2</sub> Sn(OCH <sub>2</sub> CH <sub>2</sub> NH <sub>2</sub> ) <sub>2</sub>	0.36	5.01	21.09	73.53	72.5
8	Bu <sub>2</sub> SnO(CH <sub>2</sub> ) <sub>2</sub> NH(CH <sub>2</sub> ) <sub>2</sub> O	3.56	20.57	41.58	34.28	34.3
9	Bu <sub>2</sub> SnOCH <sub>2</sub> CH <sub>2</sub> O	0.72	10.81	29.27	59.20	57.3
10	Bu <sub>2</sub> Sn(OC <sub>6</sub> H <sub>5</sub> ) <sub>2</sub>	0.89	10.28	26.40	62.43	61.3
11	Bu <sub>2</sub> Sn(OC <sub>6</sub> H <sub>4</sub> Cl- <i>p</i> ) <sub>2</sub>	0.98	10.35	26.49	62.19	64.3
12	Bu <sub>2</sub> Sn(OC <sub>6</sub> H <sub>4</sub> NO <sub>2</sub> - <i>p</i> ) <sub>2</sub>	14.15	28.58	42.34	14.93	16.8
13	Bu <sub>2</sub> SnOC <sub>6</sub> H <sub>4</sub> CH <sub>2</sub> O- <i>o</i>	1.85	14.30	33.08	50.77	49.7
14	Bu <sub>2</sub> Sn(OCH <sub>2</sub> CH <sub>2</sub> Cl) <sub>2</sub>	5.27	28.92	53.29	12.52	12.1
15	Bu <sub>2</sub> SnO	1.67	14.20	31.90	52.24	52.1
16	Oct <sub>2</sub> Sn(O(CH <sub>2</sub> ) <sub>3</sub> CH <sub>3</sub> ) <sub>2</sub>	1.68	8.26	26.64	63.42	62.0
17	Oct <sub>2</sub> Sn(O(CH <sub>2</sub> ) <sub>4</sub> CH <sub>3</sub> ) <sub>2</sub>	1.17	7.20	23.58	68.05	62.6
18	Oct <sub>2</sub> Sn(O(CH <sub>2</sub> ) <sub>5</sub> CH <sub>3</sub> ) <sub>2</sub>	2.22	9.64	25.96	62.18	59.1
19	Oct <sub>2</sub> Sn(O(CH <sub>2</sub> ) <sub>6</sub> CH <sub>3</sub> ) <sub>2</sub>	0.94	9.49	27.24	62.32	60.4
20	Oct <sub>2</sub> Sn(O(CH <sub>2</sub> ) <sub>7</sub> CH <sub>3</sub> ) <sub>2</sub>	2.31	10.14	26.49	61.06	62.6
21	Oct <sub>2</sub> Sn(O(CH <sub>2</sub> ) <sub>9</sub> CH <sub>3</sub> ) <sub>2</sub>	0.55	8.76	26.36	64.33	61.6
22	Oct <sub>2</sub> Sn(OCH <sub>2</sub> CH <sub>2</sub> NH <sub>2</sub> ) <sub>2</sub>	0.56	5.13	17.04	77.27	75.8
23	Oct <sub>2</sub> SnO(CH <sub>2</sub> ) <sub>2</sub> NH(CH <sub>2</sub> ) <sub>2</sub> O	1.70	7.77	25.83	64.71	65.4
24	Oct <sub>2</sub> SnO	1.91	6.81	23.98	67.30	65.3

<sup>a</sup>  $T = 70.0 \pm 0.1$  °C; solvent medium, MeOH; [TP]<sub>0</sub> = 12.47 mM.<sup>b</sup> Based on the equation: % Glycerol = 100 – [A + B + C].<sup>c</sup> Titrimetric method (Ref. 28).

under reduced pressure in a vacuum desiccator. Sufficient BSTFA (0.2 ml) was added to the residue in each of the vials, and the capped contents were then heated to 100 °C for 3 min with gentle shaking, followed by cooling to room temperature. Next, 0.04 ml of the 50.0 mM triacontane standard was added and the contents of each vial were made up to 2.0 ml with chloroform to yield the standard solutions. Chromatograms were run on 1.0- $\mu$ l samples of the standard solutions in replicate. Sharp and well-resolved peaks characterized the chromatogram; typical retention times (min) for the components are as follows: MeP 1.03, MoP 3.59, triacontane 4.70, DiP 6.77, TP 9.26. The less dominant<sup>26</sup> positional isomers 1,2-DiP and 2-MoP were not detected. The peak area ratio of the individual components relative to that of the internal standard,  $A_c/A_s$ , was computed and plotted against concentration to yield the standard calibration graphs for each of the components.

The calibration graphs showed good linearity and reproducibility under the optimum column operating conditions, with high correlation coefficients of 0.995 for MeP, 0.999 for MoP, 0.997 for DiP and 0.971 for TP. The minimum detection limit for the sample constituents was *ca* 40 ng (signal intensity: 3  $\times$  baseline noise). Based on the slopes of the regression lines, the concentrations of the components at various times during a kinetic run could be calculated from Eqns [2]–[5].

$$[\text{MeP}]_t = (A_c/A_s)_t/0.776 \quad [2]$$

$$[\text{MoP}]_t = (A_c/A_s)_t/0.890 \quad [3]$$

$$[\text{DiP}]_t = (A_c/A_s)_t/1.228 \quad [4]$$

$$[\text{TP}]_t = (A_c/A_s)_t/0.951 \quad [5]$$

Table 2 illustrates such data for sample aliquots

**Table 2** Peak area ratios ( $A_c/A_s$ )<sup>a</sup> and corresponding concentrations of unreacted tripalmitin and its product fractions at various time intervals using 1,1-dibutyl-5-aza-2,8-dioxo-1-stannacyclo-octane as catalyst<sup>b</sup>

Time (h)	Peak area ratio $A_c/A_s$				Concentration (mM)			
	TP	DiP	MoP	MeP	TP	DiP	MoP	MeP
0.5	1.89	0.37	0.02	0.13	7.55 (7.62)	1.23 (0.43)	0.11	0.67
1.0	1.98	0.45	0.04	0.23	7.90 (7.34)	1.51 (0.81)	0.18	1.17
1.5	1.75	0.49	0.05	0.32	7.00 (7.07)	1.65 (1.16)	0.21	1.62
2.0	1.60	0.55	0.06	0.46	6.39 (6.82)	1.85 (1.47)	0.26	2.35
2.5	1.73	0.62	0.07	0.54	6.91 (6.57)	2.09 (1.75)	0.34	2.72
3.0	1.45	0.64	0.09	0.63	5.81 (6.33)	2.15 (1.99)	0.40	3.21
3.5	1.69	0.72	0.10	0.79	6.74 (6.10)	2.41 (2.21)	0.46	3.99
4.0	1.38	0.73	0.11	0.81	5.51 (5.88)	2.46 (2.40)	0.52	4.11
5.0	1.51	0.80	0.14	1.04	6.04 (5.46)	2.70 (2.70)	0.65	5.25
6.0	1.01	0.72	0.17	1.20	4.03 (5.07)	2.41 (2.93)	0.79	6.10
7.0	1.12	0.77	0.17	1.24	4.46 (4.71)	2.60 (3.09)	0.79	6.31
8.0	1.20	0.91	0.22	1.55	4.81 (4.38)	3.06 (3.19)	1.01	7.87
10.0	0.94	0.87	0.27	2.03	3.76 (3.78)	2.92 (3.25)	1.25	10.31
12.0	0.85	0.91	0.32	2.40	3.39 (3.26)	3.05 (3.18)	1.48	12.17
24.0	0.39	0.78	0.47	3.52	1.56 (1.34)	2.61 (1.88)	2.16	17.85

<sup>a</sup>  $A_c$  = area of unreacted tripalmitin or product fraction peak;  $A_s$  = area of internal standard (triacontane) peak. Each set of entries is the average of 2–3 determinations of sample takes at various time intervals; iterative analysis values are quoted in parentheses

<sup>b</sup> Reaction conditions: MeOH/THF 3:2 (v/v);  $T = 70.0 \pm 0.1$  °C;  $[TP]_0 = 9.83$  mM.

analysed at various times for the reaction catalysed by dibutyl-5-aza-2,8-dioxo-1-stannacyclo-octane (**8**).

### Kinetic studies

In a typical experiment, 1.01 g (1.25 mmol) of tripalmitin (TP) was added to a three-necked round-bottomed flask containing 150.0 ml (3.75 mol) of methanol and 100.0 ml of tetrahydrofuran (THF). The flask was fitted with a condenser and a drying tube and placed in a controlled temperature bath ( $70.0 \pm 0.1$  °C). To the flask was added 0.004 g of the chosen catalyst (corresponding to 1.0 mol% relative to TP) and the time was recorded at the start of the reaction. Sample aliquots (0.5 ml) were withdrawn periodically from the flask at various time intervals as the reaction progressed, quickly chilled, concentrated, derivatized with BSTFA, and made up to a final volume of 2.0 ml with added internal standard. Portions (1.0  $\mu$ l) were then injected into the GC for analysis of the unreacted tripalmitin and of the products formed. The analysis was replicated. The reaction was followed to at least three half-lives.

For the reaction using catalyst **8**, the kinetics were also followed at 2.0 and 3.0 mol% catalyst concentrations, as well as at three other temperatures ( $50.0 \pm 0.1$ ,  $60.0 \pm 0.1$  and  $80.00 \pm 0.1$  °C).

For the 3.0 mol% case, the initial tripalmitin concentration was set close to 10.0 mM. Figure 1 sketches the kinetic profile for this reaction based on the compositional analysis data (Table 2) procured at various time intervals. The smooth decrease of TP with time is strongly indicative of pseudo first-order kinetics; other features in the graph (see the Results and Discussion section) point to the stepwise reaction scheme in Eqn [6].



Computer iterative methods (non-linear least-squares analysis) were used to estimate  $k_1$  and  $k_2$ , and  $k_3$  was estimated by the Newton–Raphson technique. Details of these techniques can be found, for example, in Ref. 27.

### Evaluation of relative efficacy of catalysts

This study, which preceded the kinetic work, was performed in a methanolic medium with each of the 25 diorganotin compounds at a bath temperature of  $70.0 \pm 0.1$  °C. The catalyst concentration was set at 3.0 mol% with respect to the tripalmitin. Comparison of catalytic efficacy was based on the estimation of the yield of the glycerol product

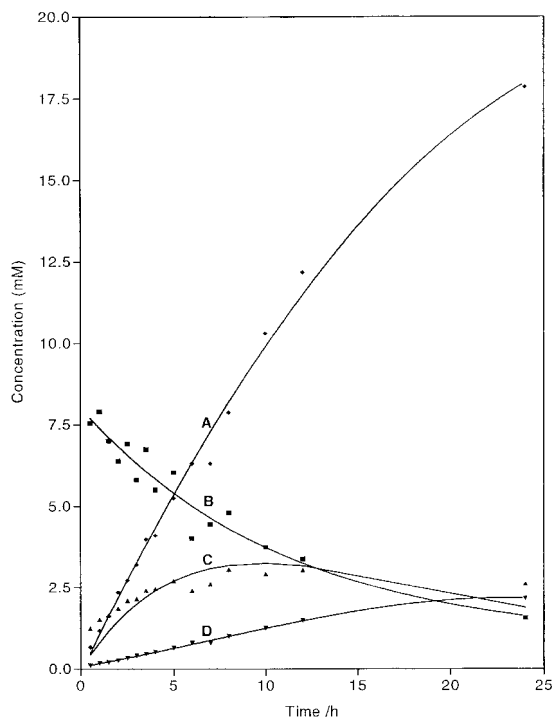


**Figure 1** Concentration–time plots of tripalmitin and its methanolysis products catalysed by 3.0 mol% of **8** at  $70.0 \pm 0.1$  °C (A, MeP; B, TP; C, DiP; D, MoP).

formed at the end of 24 h of the transesterification reaction. This was accomplished directly by duplicating a titrimetric method<sup>28</sup> as well as indirectly by GC analysis of the other product components. It is seen from the data in Table 1 that both of these methods provide consistent estimates of the glycerol yields.

## RESULTS AND DISCUSSION

### Evaluation of catalytic properties

Based on the glycerol yields, the dioctyltin alkoxides were found to be more effective catalysts than the dibutyltin alkoxides (Table 1). In Fig. 2 the product compositional yields are plotted against the carbon chain length of the alkoxy fragment in the dibutyltin bis(alkoxide) catalyst series. The yields decreased steadily with increasing chain length of the alkoxy fragment. The reduction was *ca* 7.2% in

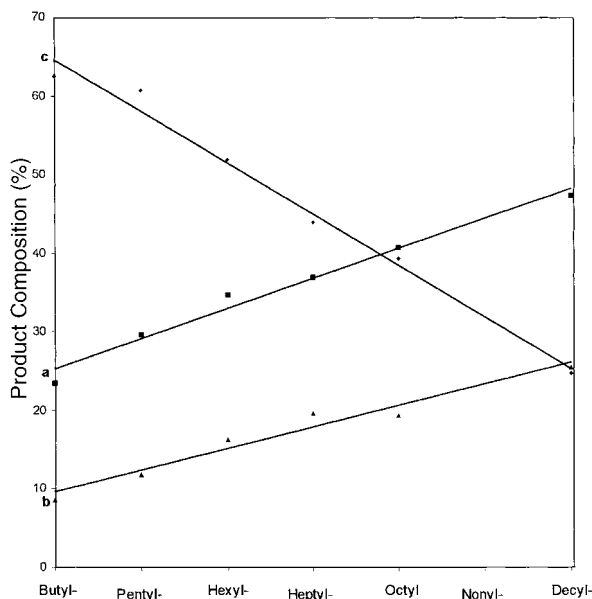


**Figure 2** Variation of product compositional yields with carbon chain length of the alkoxy fragment in dibutyltin bis(alkoxide) catalysts (a, MoP; b, DiP; c, glycerol).

glycerol yield for each  $\text{CH}_2$  increment in the alkoxide chain.

Not unexpectedly, the decline in glycerol yields resulted in a build-up of the mono- and dipalmitins, and hence plots for these (Fig. 2, curves a, b) have slopes opposite to that of curve c. The results suggest that the activity of diorganotin bis(alkoxides) was influenced by the nature of both the alkyl and alkoxy groups.

Differences in glycerol yields appeared to be minimal with butyl- and octyl-tin alkoxides of diethanolamine, but were rather significant (47%) when the alkoxy function is derived from ethanolamine. For the pair of catalysts  $\text{Bu}_2\text{Sn}(\text{OCH}_2\text{CH}_2\text{NH}_2)_2$  and  $\text{Bu}_2\text{Sn}(\text{OCH}_2\text{CH}_2\text{Cl})_2$  the difference in glycerol yields was about 60%, attesting to the rather profound influence of substituents in the alkoxy residue on the overall catalytic activity.

The activities of the cyclic dibutyltin alkoxides derived from the bifunctional ligands ethylene glycol (**9**), 2-hydroxybenzyl alcohol (**13**) and diethanolamine (**8**) decreased with increasing chelate ring size. Surprisingly, 1,1-dioctyl-5-aza-2,8-dioxo-1-stannacyclooctane (**23**), which contains an eight-membered ring, was found to be catalytically more efficient (glycerol yield *ca* 65%)

**Table 3** Product composition analysis at the end of 24 h of the transesterification reaction of tripalmitin conducted in MeOH–CHCl<sub>3</sub> (1:1, v/v) medium at 65.0 ± 0.1 °C in the presence of 1.0 wt% catalyst with respect to tripalmitin<sup>a</sup>

Catalyst	Unreacted TP (%) <sup>b</sup> (A)	DiP (B)	MoP (C)	Product (%)	
				Glycerol	
				Direct estimate	Indirect estimate
BuSnCl <sub>3</sub>	65.5	12.1	6.1	14.6	16.3
Bu <sub>2</sub> SnCl <sub>2</sub>	nil	19.3	42.2	39.8	38.5
Bu <sub>3</sub> SnCl	68.0	12.7	5.6	11.6	13.7
Bu <sub>2</sub> SnO	nil	7.7	22.5	71.5	69.8
H <sub>2</sub> SO <sub>4</sub>	48.0	3.6	1.9	44.2	46.5
Uncatalysed	62.8	19.8	10.4	8.8	7.0

<sup>a</sup> Abstracted in part from E.S Looi and V. G. Kumar Das (unpublished results) and Ref. 29<sup>b</sup> Relative to [TP]<sub>0</sub> = 3.15 mM.<sup>c</sup> Based on the equation: % Glycerol = 100 – [A + B + C].

than the corresponding dibutyltin analogue (glycerol yield 34.3%) or 2,2-dibutyl-2-stanna-1,3-dioxolane (**9**) (glycerol yield 57.3%).

The dibutyltin bis(phenoxides) were comparable in their activity with the dioctyltin bis(alkoxides). Interestingly, however, Bu<sub>2</sub>Sn(OC<sub>6</sub>H<sub>4</sub>NO<sub>2</sub>-*p*)<sub>2</sub> (glycerol yield 16.8%) manifested a significantly lower activity than Bu<sub>2</sub>Sn(OC<sub>6</sub>H<sub>4</sub>Z-*p*)<sub>2</sub> (Z = H or Cl) (glycerol yields 61.3% and 64.3%, respectively).

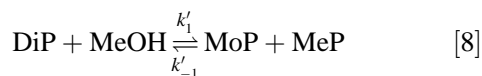
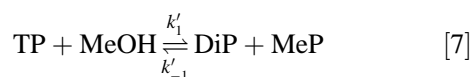
Table 1 also includes data for the diorganotin oxides. Oct<sub>2</sub>SnO (**24**) was marginally more active than Bu<sub>2</sub>SnO (**15**). Dibutyltin oxide also featured in a limited study with BuSnCl<sub>3</sub>, Bu<sub>2</sub>SnCl<sub>2</sub>, Bu<sub>3</sub>SnCl and sulphuric acid as catalysts for the transesterification of tripalmitin conducted in MeOH/CHCl<sub>3</sub> (1:1, v/v) medium at 65.0 ± 0.1 °C. The data in Table 3 attest to the better catalytic property of diorganotins.<sup>29</sup>

## Kinetic studies

For the purpose of the kinetic studies, five diorganotin compounds (**8**, **10**, **11**, **13** and **24**) were selected. The catalyst concentration was set at 1.0 mol% with respect to tripalmitin (TP), and the experiments were generally performed at the bath temperature of 70.0 ± 0.1 °C. In the particular case involving catalyst **8**, the reaction was also performed at three other temperatures (50, 60 and 80 °C) for each of two catalytic concentrations, namely 1.0 and 3.0 mol% relative to tripalmitin.

For the case of the reaction catalysed by **8** at 70.0 ± 0.1 °C, the concentration–time plot obtained

is depicted in Fig. 1. A half-life of *ca* 9.5 h is inferred for the reaction. The concentration of the methyl palmitate product also increased smoothly with respect to time, almost reaching the theoretical yield in *ca* 48 h. The concentration of dipalmitin reached a maximum corresponding to 3.3 mM in approximately 10 h, and subsequently decreased. The maximum concentration of mono-palmitin at 2.0 mM was attained in almost 24 h, at which point the dipalmitin concentration was minimal. These trends suggest a stepwise reaction for the transesterification of tripalmitin as indicated in Eqns [7]–[9], where *k*'<sub>1</sub>, *k*'<sub>2</sub> and *k*'<sub>3</sub> represent the rate constants of the forward reactions, and *k*'<sub>–1</sub>, *k*'<sub>–2</sub> and *k*'<sub>–3</sub> those of the reverse reactions.



Noting that the reagent methanol was present in excess, and assuming that under the conditions of the experiment the reaction equilibria were largely shifted in the direction of the products, the rate equations [10]–[13] apply,

$$\frac{-d[\text{TP}]}{dt} = k_1[\text{TP}] \quad [10]$$

$$\frac{d[\text{DiP}]}{dt} = k_1[\text{TP}] - k_2[\text{DiP}] \quad [11]$$

$$\frac{d[\text{MoP}]}{dt} = k_1[\text{DiP}] - k_3[\text{MoP}] \quad [12]$$

$$\frac{d[\text{MeP}]}{dt} = k_1[\text{TP}] + k_2[\text{DiP}] + k_3[\text{MoP}] \quad [13]$$

where  $k'_1 = k'_{[1]} [\text{MeOH}]$ ,  $k_{[2]} = k'_{[2]} [\text{MeOH}]$  and  $k_{[3]} = k'_{[3]} [\text{MeOH}]$

In line with this assumption is the non-detection of either dipalmitin or tripalmitin in the experiment on the methanolysis of monopalmitin (*vide infra*). The integrated form of Eqn [10] may be given as Eqn [14],

$$[\text{TP}]_t = [\text{TP}]_0 \exp(-k_1 t) \quad [14]$$

where  $[\text{TP}]_t$  is the concentration of tripalmitin at a given time  $t$ , and  $[\text{TP}]_0$  is its initial concentration. The plot of  $\ln[\text{TP}]_0/[\text{TP}]_t$  vs time ( $t$ ) is thus expected to be linear, and this was indeed observed, yielding a value of  $0.089 \pm 0.006 \text{ h}^{-1}$  for the rate constant,  $k_1$ .

Treatment of the raw data points by non-linear least-squares analysis yielded best-fit values for the tripalmitin concentrations at various times, and the rate constant,  $k_1$ , thus computed was  $0.074 \pm 0.007 \text{ h}^{-1}$ .

Incorporating Eqn [14] into Eqn [11] we have the exact differential equation [15].

$$\exp(k_2 t) \frac{d[\text{DiP}]}{dt} + \exp(k_2 t) [\text{DiP}] k_2 = k_1 [\text{TP}]_0 \exp(k_2 - k_1) t \quad [15]$$

Integrating this equation under the limits  $t = 0$ ,  $[\text{DiP}] = 0$  we obtain Eqn [16].

$$[\text{DiP}]_t = \frac{k_1 [\text{TP}]_0}{k_2 - k_1} [\exp(-k_1 t) - \exp(-k_2 t)] \quad [16]$$

Feeding the calculated value of  $k_1$  and the observed values of  $[\text{DiP}]_t$  at various time intervals into Eqn [16], and performing the iterative analysis on the data set (see Table 2 in the Experimental section), afforded best-fit values for  $k_1$  and  $k_2$  of  $k_1 = 0.092 \pm 0.009 \text{ h}^{-1}$  and  $k_2 = 0.113 \pm 0.024 \text{ h}^{-1}$ .

It is to be noted that Eqn [16] involves a difference between two exponential terms, which in a theoretical sense should have a maximum value.  $[\text{DiP}]_{\text{max}}$  occurs at time  $t_{\text{max}}$  (Eqn [17]),

given by Eqn [18].

$$t_{\text{max}} = \frac{\ln(k_2/k_1)}{k_2 - k_1} \quad [17]$$

$$[\text{DiP}]_{\text{max}} = [\text{TP}]_0 [k_2/k_1]^{k_2/(k_1 - k_2)} \quad [18]$$

With reference to curve **C** in Fig 1 which depicts the variation of  $[\text{DiP}]$  with time, it is seen that the concentration of  $[\text{DiP}]$  reached a maximum at *ca* 10 h following commencement of reaction; this corresponded to a concentration of *ca* 3.3 [m][M]. These data compare rather favourably with the values of 10 h and 3.25 [m][M] calculated on the basis of Eqn [18], which attests to the correctness of the consecutive reaction pathway envisaged for the transesterification reaction.

Whereas the value of  $k_2$  calculated from Eqn [16] is necessarily dependent on the number of data points included in the calculation, the use of Eqn [18] requires significantly fewer data points to define  $[\text{DiP}]_{\text{max}}$ . Feeding  $k_1$ ,  $[\text{DiP}]_{\text{max}}$ ,  $[\text{TP}]_0$  and estimated values of the  $k_2/k_1$  ratio ( $\equiv K$ ) into Eqn [18] and performing the iterative analysis, best-fit values of  $K = k_2/k_1 = 1.2304$  and  $k_2 = 0.0908 \text{ h}^{-1}$  were obtained.

The concentration of monopalmitin,  $[\text{MoP}]$ , at a given time  $t$  may be obtained by integrating Eqn [12] under the limits  $t = 0$ ,  $[\text{MoP}] = 0$ . This yields Eqn [19].

$$[\text{MoP}]_t = [\text{TP}]_0 k_1 k_2 \left[ \frac{\exp(-k_1 t)}{(k_2 - k_1)(k_3 - k_1)} - \frac{\exp(-k_2 t)}{(k_2 - k_1)(k_3 - k_2)} + \frac{\exp(-k_3 t)}{(k_3 - k_1)(k_3 - k_2)} \right] \quad [19]$$

The rate constant  $k_3$  may be computed by means of the Newton-Raphson iteration technique<sup>27</sup> using the values of  $k_1$  and  $k_2$  previously derived. Feeding the respective observed values of  $[\text{MoP}]_t$  at various times  $t$  into Eqn [19] and performing the iterative analysis yields a  $k_3$  value for each data set. Of these, the values obtained for the initial stage (0.5–6 h) of the reaction were widely divergent and therefore were discarded. A probable reason for the divergence was that the tripalmitin used in the transesterification was only 95% pure and could conceivably have contained either or both of di- and mono-palmitins. The average of the  $k_3$  values for the reaction period from 7 to 24 h was  $0.124 \pm 0.014 \text{ h}^{-1}$ .

**Table 4** Estimation of  $[TP]_0$  using Eqn [23]

Time (h)	0.5	1.0	1.5	2.0	2.5	3.0	3.5	4.0	5.0	7.0	8.0	10.0	12.0	24.0
$[TP]_0$ (mM)	8.63	9.36	8.71	8.50	9.32	8.45	9.83	8.70	9.81	8.57	9.81	9.56	9.97	9.96

The rate of methyl palmitate formation may be conveniently addressed in terms of mass balance. A mass balance is defined by the condition  $[TP]_0 = [TP]_t + [DiP]_t + [MoP]_t + [Gly]_t$ , or stated differently, there must be no net change in the rate of variation of  $[TP]_t$  with respect to that of the ester products. From Eqns [10]–[13], it is evident that this condition is satisfied by the stoichiometric equation [20].

$$3 \frac{d[TP]}{dt} + 2 \frac{d[DiP]}{dt} + \frac{d[MoP]}{dt} + \frac{d[MeP]}{dt} = 0 \quad [20]$$

Rewriting Eqn [20] in integrated form, we have Eqn [21].

$$3 \int_{[TP]_0}^{[TP]_t} d[TP] + 2 \int_0^{[DiP]_t} d[DiP] + \int_0^{[MoP]_t} d[MoP] + \int_0^{[MeP]_t} d[MeP] = 0 \quad [21]$$

Integrating Eqn [21] under the limits indicated leads to Eqn [22],

$$3([TP]_t - [TP]_0) + 2[DiP]_t + [MoP]_t + [MeP]_t = 0 \quad [22]$$

which may be rearranged to Eqn [23].

$$[MeP]_t = 3\{[TP]_0 - [TP]_t\} - 2[DiP]_t - [MoP]_t \quad [23]$$

From the tabulated data in Table 2, we note that at  $t = 8$  h (say),  $[MeP] = 7.87$  mM, and the corresponding values of  $[TP]_t$ ,  $[DiP]_t$  and  $[MoP]_t$  are respectively 4.81, 3.06 and 1.01 mM;  $[TP]_0 = 9.83$  mM. The calculated value of  $[MeP]_t$  from Eqn [23] using the above inputs is 7.94 mM. This is in close agreement with the observed value. Equation [23] also allows  $[TP]_0$  to be estimated at any given time  $t$  from measurements of  $[TP]_t$  and the associated product concentrations. Thus, for the case at hand,

$$[TP]_0 = 4.81 + 2 \frac{(3.06)}{3} + \frac{(1.01)}{3} + \frac{(7.87)}{3} = 9.81 \text{ mM}$$

This value is in excellent agreement with the actual

initial tripalmitin concentration of 9.83 mM. The calculated values of  $[TP]_0$  obtained using Eqn [23] at different times during the course of the reaction are compared in Table 4. The near-constancy of the values attests strongly to a mechanism for the methanolysis reaction based on the consecutive reaction pathway. This also rules out the presence of any competing 'shunt' reaction such as was described by Freedman *et al.*<sup>30</sup> for the methanolysis of soybean oil catalysed by sodium methoxide in which one molecule of the triglyceride was envisaged to be attacked simultaneously by three molecules of methanol to give the products.

Pseudo first-order kinetics was also observed for the methanolysis reactions conducted separately on dipalmitin and monopalmitin using catalyst **8** under similar experimental conditions. The plots of  $\ln[DiP]_0/[DiP]_t$  vs time ( $t$ ) and  $\ln[MoP]_0/[MoP]_t$  vs  $t$  were linear, yielding the values  $k_2 = 0.979 \pm 0.013 \text{ h}^{-1}$  and  $k_3 = 1.136 \pm 0.007 \text{ h}^{-1}$ , respectively. Iterative analysis of the data set for dipalmitin yielded  $k_2 = 0.561 \pm 0.006 \text{ h}^{-1}$  and  $k_3 = 0.555 \pm 0.007 \text{ h}^{-1}$ , whereas that for monopalmitin gave  $k_3 = 1.153 \pm 0.005 \text{ h}^{-1}$ . These values, however, are higher than those estimated by the iterative method from the methanolysis of tripalmitin ( $k_2 = 0.113 \pm 0.024 \text{ h}^{-1}$ ;  $k_3 = 0.124 \pm 0.014 \text{ h}^{-1}$ ). The reason for this resides in the fact that the rate data were not strictly comparable as the effective catalyst/substrate ratio differed for the three cases.

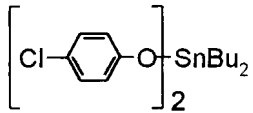
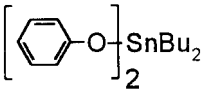
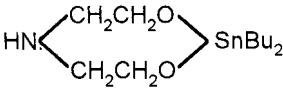
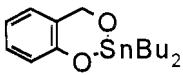
Table 5 compares the rate constants for the transesterification of tripalmitin with each of five selected organotin catalysts. Based on the half-lives for tripalmitin conversion, the order of catalytic activity was **11** > **10** > **8** >> **24** >> **13**

## Effects of variation in catalyst concentration

For catalyst **8**, the transesterification reaction was also conducted at two other catalyst concentrations, namely 2.0 and 3.0 mol%, relative to tripalmitin. The results are summarized in Table 6(a). A six-fold increase in the rate resulted when the catalyst concentration was raised from 1.0 to 3.0 mol%. The half-life for the uncatalysed reaction was 23.1 h.



**Table 5** Rate constants for the methanolysis of tripalmitin at  $70.0 \pm 0.1$  °C catalysed by each of five diorganotin catalysts (catalyst/tripalmitin ratio = 1.0 mol%)

Catalyst <sup>a</sup>	Catalyst no.	$k_1$ (h <sup>-1</sup> )	$k_2$ (h <sup>-1</sup> )	$k_3$ (h <sup>-1</sup> )	$t_{1/2}$ (h)
	<b>11</b>	$0.095 \pm 0.016$	$0.116 \pm 0.025$	$0.285 \pm 0.154$	7.29
	<b>10</b>	$0.085 \pm 0.008$	$0.102 \pm 0.019$	$0.185 \pm 0.097$	8.15
	<b>8</b>	$0.074 \pm 0.007$	$0.113 \pm 0.024$	$0.124 \pm 0.014$	9.37
	<b>13</b>	$0.031 \pm 0.006$	$0.056 \pm 0.011$	$0.064 \pm 0.015$	22.36
Oct <sub>2</sub> SnO	<b>24</b>	$0.041 \pm 0.002$	$0.069 \pm 0.010$	$0.086 \pm 0.007$	16.91

<sup>a</sup>  $t_{1/2} = 0.693/k_1$ 

### Effects of variation in solvent composition

The transesterification reaction using catalyst **8** was also conducted in the mixed solvent system [CHCl<sub>3</sub>]-[MeOH] (2:3, v/v) to effect comparisons with the THF-MeOH (2:3, v/v) system used in the preceding experiments. The derived rate constants  $k_1$ ,  $k_2$  and  $k_3$  are compared in Table 6(b). The results show that the transesterification reaction proceeded faster in the presence of THF than in the presence of chloroform.

### Effects of temperature variations

The transesterification reaction catalysed by **8** was also performed at four different temperatures in MeOH-THF (3:2, v/v) at two catalyst concentrations (1.0 and 3.0 mol%). The results are summarized in Table 6(c). A near-doubling of the three rate constants was observed for each 10 °C rise in

temperature from 50 to 80 °C for the case where the catalyst concentration is 1.0 mol%. The rate constants at  $80.0 \pm 0.1$  °C were comparable in magnitude with those obtained at  $70.0 \pm 0.1$  °C using Bu<sub>2</sub>Sn(OC<sub>6</sub>H<sub>4</sub>Cl-*p*)<sub>2</sub> as the catalyst (see Table 5). The increases were less substantial, however, at the catalyst loading of 3.0 mol%.

Arrhenius plots of the rate data in Table 6(c) yield the activation energy  $E_a$  values in Table 7, which includes the entropies and free energies of activation. The data reveal that there were minor changes in the entropies of activation between the uncatalysed, the 1.0 mol% catalysed and the 3.0 mol% catalysed reactions. The presence of the 1,1-dibutyl-5-aza-2,8-dioxo-1-stannacyclo-octane catalyst was particularly effective in lowering the enthalpy of activation, while keeping the entropy virtually unchanged. This unique characteristic in bringing down the highest energy barrier in a reaction while maintaining the molecular 'surroundings' virtually unchanged is particularly

**Table 6** Effects of variations in catalyst concentration, solvent composition and temperature on rate constants<sup>a</sup>

	$k_1$ (h <sup>-1</sup> )	$k_2$ (h <sup>-1</sup> )	$k_3$ (h <sup>-1</sup> )	$t_{1/2}$ (h)
(a) <i>Catalyst conc</i> <sup>b</sup> (mol%)				
Uncatalysed	0.030 ± 0.002	0.065 ± 0.014	0.050 ± 0.100	23.10
1.0	0.074 ± 0.007	0.113 ± 0.024	0.124 ± 0.014	9.37
2.0	0.147 ± 0.008	0.383 ± 0.085	0.248 ± 0.083	4.72
3.0	0.445 ± 0.012	1.089 ± 0.102	0.523 ± 0.130	1.56
(b) <i>Solvent system</i> <sup>b, c</sup>				
THF/MeOH (2/3 v/v)	0.074 ± 0.007	0.113 ± 0.024	0.124 ± 0.01	9.37
CHCl <sub>3</sub> /MeOH (2/3 v/v)	0.026 ± 0.002	0.034 ± 0.010	0.053 ± 0.005	26.66
(c) <i>Temperature</i> (°C) <sup>c, d</sup>				
50.0 ± 0.1	0.019 ± 0.001 (0.030 ± 0.002)	0.028 ± 0.005 (0.083 ± 0.022)	0.030 ± 0.003 (0.061 ± 0.019)	36.48 (23.10)
60.0 ± 0.1	0.039 ± 0.005	0.054 ± 0.009	0.066 ± 0.010	17.77
70.0 ± 0.1	0.074 ± 0.007 (0.089 ± 0.006)	0.113 ± 0.024 (0.133 ± 0.037)	0.124 ± 0.014 (0.270 ± 0.058)	9.37 (7.79)
80.0 ± 0.1	0.103 ± 0.007 (0.124 ± 0.007)	0.135 ± 0.029 (0.175 ± 0.047)	0.247 ± 0.075 (0.438 ± 0.033)	6.73 (5.59)

<sup>a</sup> Catalyst, **8**.<sup>b</sup>  $T = 70.0 \pm 0.1$  °C.<sup>c</sup> 1.0 mol% catalyst relative to tripalmitin.<sup>d</sup> Values in parentheses are for 3.0 mol% catalyst relative to tripalmitin.

important in maintaining the purity and integrity of the final products. The free energy of activation,  $\Delta G^\ddagger$ , for the 1.0 mol% catalysed reaction at 70.0 °C was 115.52 kJ mol<sup>-1</sup>; varying the temperature of the reaction led to no significant change in this value.

### Chemical nature of the diorganotin alkoxide catalyst at the end of the transesterification reaction

The fate of the dialkyltin alkoxide catalyst at the end of the methanolysis reaction was of interest.

**Table 7** Variations in rate constants and related thermodynamic parameters with catalyst concentrations in the methanolysis of tripalmitin at 70.0 ± 0.1 °C (343 K)<sup>a</sup>

Catalyst/tripalmitin ratio	Thermodynamic parameters <sup>b</sup>	Reaction pathway		
		$k_1$	$k_2$	$k_3$
1.0 mol%	$E_a$ (kJ mol <sup>-1</sup> )	54.98	50.59	66.94
	$\Delta H^\ddagger_{343}$ (kJ mol <sup>-1</sup> )	52.13	47.74	64.09
	$\Delta S^\ddagger_{343}$ (J K <sup>-1</sup> mol <sup>-1</sup> )	-184.83	-194.74	-144.21
	$\Delta G^\ddagger_{343}$ (kJ mol <sup>-1</sup> )	115.52	114.54	113.55
3.0 mol%	$E_a$ (kJ mol <sup>-1</sup> )	45.37	22.67	62.06
	$\Delta H^\ddagger_{343}$ (kJ mol <sup>-1</sup> )	42.52	19.82	59.21
	$\Delta S^\ddagger_{343}$ (J K <sup>-1</sup> mol <sup>-1</sup> )	-210.93	-235.87	-153.10
	$\Delta G^\ddagger_{343}$ (kJ mol <sup>-1</sup> )	114.87	100.72	111.72
Uncatalysed	$E_a$ (kJ mol <sup>-1</sup> )	64.70	52.79	47.45
	$\Delta H^\ddagger_{343}$ (kJ mol <sup>-1</sup> )	61.85	49.94	44.60
	$\Delta S^\ddagger_{343}$ (J K <sup>-1</sup> mol <sup>-1</sup> )	-161.83	-192.17	-208.99
	$\Delta G^\ddagger_{343}$ (kJ mol <sup>-1</sup> )	117.36	115.85	116.28

<sup>a</sup> Catalyst, 1,1-dibutyl-5-aza-2,8-dioxo-1-stannacyclo-octane.<sup>b</sup>  $E_a$ , Arrhenius activation energy;  $\Delta H^\ddagger$ , enthalpy of activation;  $\Delta S^\ddagger$ , entropy of activation;  $\Delta G^\ddagger$ , free energy of activation.

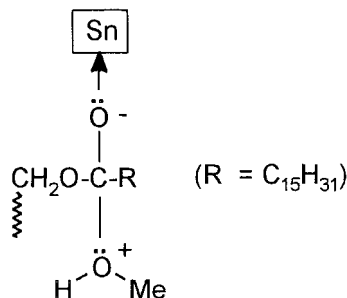
This was probed using  $^{119}\text{Sn}$  NMR spectroscopic analysis for two cases involving catalysts **8** and **11**.

A semi-solid residue containing the catalyst was obtained in the reaction pot when the methanol–THF medium was removed using a rotary evaporator. A portion of this residue, while still warm and homogeneous, was taken up in a small amount of  $\text{CDCl}_3$  for the NMR analysis.

The spectrum of the pot residue containing catalyst **8** showed a single tin resonance at  $-133.6$  ppm (relative to  $\text{Me}_4\text{Sn}$ ). The pure catalyst showed a chemical shift of  $-108.6$  ppm in  $\text{CDCl}_3$ , which shifted only marginally upfield ( $3\text{--}5$  ppm) upon co-addition of methyl palmitate, but more strongly when a small amount of *N,N*-dimethylformamide (DMF) ( $\delta -120.7$  ppm) or methanol ( $\delta -131.5$  ppm) was added, attesting to a coordinative interaction of these donor molecules with tin. Indeed, the pronounced sensitivity of the  $^{119}\text{Sn}$  chemical shifts of most organotin compounds to solvent effects is well known.<sup>31</sup> The somewhat larger shift occasioned here by the weaker Lewis base, methanol, suggests that the latter may also be simultaneously participating in hydrogen bonding with the oxygen atoms of the dioxastannolane. However, when the pure catalyst was recovered from methanol after 24 h reflux in it, and its spectrum was re-run in  $\text{CDCl}_3$  following vacuum drying, it registered a tin chemical shift of  $-111.2$  ppm. It may thus be inferred that the structure of **8** remained essentially unaltered following its use in the transesterification reaction. For the recovered catalyst **11**, two minor peaks at  $-197.7$  and  $-210.5$  ppm were noted along with the major resonance at  $-178.5$  ppm in  $\text{CDCl}_3$ . The chemical shift of the major peak differed little from that of the pure compound in either  $\text{CDCl}_3$  or  $\text{CDCl}_3\text{--MeOH}$ , but the  $-197.7$  ppm peak coincided with the trace peak also discerned for the pure compound in the mixed solvent. We attribute the minor peak to the development of a distannoxane or associated structure for the phenoxide. Indeed, two tin sites are often observed in the solution ( $\text{CDCl}_3$ )  $^{119}\text{Sn}$  NMR spectra of many non-cyclic diorganotin bisalkoxides. Thus, catalyst **11** may also be considered largely to retain its chemical integrity. It is noteworthy that no peaks corresponding to the formation of dibutyltin bismethoxide were observed in the spectral analysis of the pot residue in either case.

While it is clear that the transesterification reaction proceeds faster in the presence of the tin compounds, the mechanism of the catalytic process can only remain conjectural at this point. A possible

pathway involves the intermediary structure shown below



where the carbonyl oxygen of the ester group is coordinated to tin and the methanol is bonded to the electron-deficient carbonyl carbon. This leads to the formation of tetrahedral carbon at the reaction site. The subsequent expulsion of the glyceroxyl moiety from this structure yields methyl palmitate. Further experiments designed to test this hypothesis are in progress.

**Acknowledgements** The authors thank Dr Niyaz Khan for valuable discussions, and the National Science Council for generous support of the research under IRPA Grant 2-07-04-06. The first author is grateful to the University of Malaya for the tenure of a tutorship at the Department of Chemistry.

## REFERENCES

1. Meffert A. *J. Am. Chem. Soc.* 1985; **61**: 255.
2. Ishi Y, Takeuchi R. *Trans. ASAE* 1987; **30**: 2.
3. Masjuki H, Zaki AM, Sapuan SM. *J. Am. Oil Chem. Soc.* 1993; **70**: 1021.
4. Eckey EW. Ester interchange. In *Encyclopedia of Chemical Technology*, Vol. 5. Interscience: New York, 1950; 817.
5. Kiem GI. US Patent 2383601 1945.
6. Bradshaw GB, Meuly WC. US Patent 2271619 1942. Freedman B, Pryde EH. *Proc. Int. Conf. Veg. Oil Fuels*, Fargo ND, 1982; 117.
7. Schuchardt U, Vargas RM, Gelbard G. *J. Mol. Catal. A: Chemical* 1995; **99**: 65; Schuchardt U, Vargas RM, Gelbard G. *J. Mol. Catal. A: Chemical* 1996; **109**: 37.
8. Schuchardt U, Lopes OC. *J. Am. Oil Chem. Soc.* 1988; **65**: 1940; Schuchardt U, Lopez OC, Braz. Pedido PIBR 02429 1982; *Chem. Abstr.* 1984; **101**: 93246.
9. Taylor F, Panzer CC, Craig JC Jr, O'Brien DJ. *Biotechnol. Bioeng.* 1986; **28**: 1318.
10. Macrae AR. In *Microbial Enzymes and Biotechnology*, Fogarty WM (ed). Applied Science: Barking, 1983; 225.
11. Poller RC, Retout SP. *J. Organomet. Chem.* 1979; **173**: C7.
12. Jones GC, Nottingham WD. (Eastman Kodak Co., PCT Int.). WO 890967 1989; *Chem. Abstr.* **112**: 178090y.

13. Wheeler EL, Jannis EH. US Patent 4263466 1981; *Chem. Abstr.* **95**: 80191n.
14. Yoshioka T, Okamura K, Kobayashi M. Japanese Patent 63198646 1988; *Chem. Abstr.* **110**: 115491t.
15. Narimatsu S, Okada M, Kimura M, Mishina H. Japanese Patent 01299263 1989; *Chem. Abstr.* **112**: 197641v.
16. Bolon DA, Gorczyca TB, Hallgren JE. US Patent 4553504 1985; 16. *Chem. Abstr.* **104**: 50677n.
17. Oda S. Japanese Patent 01311054 1989; *Chem. Abstr.* **112**: 234823d.
18. Cottman KS, Kuczkowski JA. European Patent EP 282435 1988; 18. *Chem. Abstr.* **110**: 96919v.
19. Otera J, Yano T, Kawabata A, Nozaki H. *Tetrahedron Lett.* 1986; **27**: 2383; Otera J, Dan-Oh N, Nozaki H. *J. Org. Chem.* 1991; **56**: 5307.
20. Evans CJ, Karpel S. *J. Organomet. Chem. Libr.* 1985; **16**: 1.
21. Bradshaw GB, Menley WC. US Patent 2360844 1944; Bradshaw GB, Menley WC. *Soap Sanit. Chem.* 1942; **18**: 23.
22. Feuge RO, Gros T. *J. Am. Oil Chem. Soc.* 1949; **26**: 97.
23. Lehman LW, Gauglitz EJ. *J. Am. Oil Chem. Soc.* 1966; **43**: 383.
24. Vogel. *A Textbook of Practical Organic Chemistry, Including Quantitative Organic Analysis*, 3rd edn., Longman, Green: London, 1956; 169–170.
25. Tan BK, Tan YA, Chow MC, Ariffin S, Bahrin Z. *Handbook on Triglyceride Composition and Chromatogram of Oils and Fats — Liquid Chromatograph*. Palm Oil Research Institute of Malaysia; 1984; 5.
26. Crossley A, Freeman IP, Hudson BJB, Pierce JH. *J. Chem. Soc.* 1959; 760.
27. Pennington RH. *Computer Methods and Numerical Analysis*, 2nd edn. Collier–Macmillan Canada: 1965; 286–292.
28. Shupe S. *J. Assoc. Offic. Agr. Chemists* 1943; **26**: 249.
29. Looi ES. M.Sc. Thesis, University of Malaya, 1992.
30. Freedman B, Butterfield RO, Pryde EH. *J. Am. Oil Chem. Soc.* 1986; **63**: 1375.
31. Wrackmeyer B. *Ann. Rep. NMR Spectrosc.* 1985; **16**: 73, and references therein.